Domain-Boundary Structure of Styrene–Isoprene Block Copolymer Films Cast from Solutions. 7. Quantitative Studies of Solubilization of Homopolymers in Spherical Domain Systems

Hiroshi Hashimoto, Mineo Fujimura, Takeji Hashimoto,* and Hiromichi Kawai

Department of Polymer Chemistry, Faculty of Engineering, Kyoto University, Kyoto 606, Japan. *Received December 2, 1980*

ABSTRACT: We investigated the effect of casting solvent on the spherical microdomain of a particular styrene–isoprene block polymer (SI) and the effect of blending homopolystyrene (HPS) and homopolyisoprene (HPI) on the spherical microdomain of particular SI block polymers, a particular casting solvent (toluene), good for both HPS and HPI, being used. The microdomain structure was quantitatively studied by SAXS in terms of the average interdomain distance $\bar{D}$, the domain radius $\bar{R}$, the size distribution σ_r, and the characteristic interfacial thickness ΔR of the domain-boundary region between the two coexisting microphases as a function of (i) casting solvents and (ii) volume fraction of homopolymers ψ_H in binary (HPS and SI) and ternary mixtures (HPS, HPI, and SI). The observed changes in $\bar{D}$ and $\bar{R}$ with ψ_H may be interpreted in terms of solubilization of the homopolymers into the respective phases. The interfacial thickness (ΔR) turns out to be essentially independent of casting solvents and the homopolymers blended into the block polymer. The analysis of the interfacial thickness ΔR involves a correction for the background scattering arising from the thermal diffuse scattering within each phase. A new method, based on additivity of the background scattering, is proposed to correct for the background scattering.

I. Introduction

Riess et al.,[1,2] Molau et al.,[3] and Inoue et al.[4] have studied the emulsifying effects of block and graft copolymers: the block and graft copolymers are able to restrain phase separation of a mixed system composed of the copolymers and the corresponding homopolymers into macroscopic domains, giving rise to microheterogeneous domain morphology. The emulsifying effect can be interpreted in terms of the concept of a polymeric oil-in-oil emulsion[5,6] as depicted in Figure 1, where it is shown that an emulsion of A droplets in B solution is stabilized by the A–B-type diblock polymers whose chemical junction points are preferentially located near the interface between the droplets and the matrix. The origin of the stabilizing force of the emulsion is essentially an entropic repulsion of the A- and B-block chains emanating from the peripheries of the droplets.[7,8]

Inoue et al.[4] further studied the emulsifying effect or the solubilizing effect (i.e., the ability of the block polymers to solubilize the corresponding homopolymers into the respective domains of the block polymers) as a function of molecular weight by means of electron microscopy. They found a criterion for the solubilizing effect: if the molecular weights of the homopolymers are about equal to or smaller than those of the corresponding block polymer chains, the homopolymers are solubilized into the respective domains; if the molecular weights of the homopolymers are far larger than the corresponding block molecular weights, the homopolymers tend to phase separate into each domain, i.e., the domains of the respective homopolymers and the domain of the block polymer with an inherent microdomain structure. The amount of solubilized homopolymers is qualitatively shown to affect the morphology of the binary or ternary mixtures in terms of size, shape, and long-range spatial order of the domains.

The effect of molecular weight on the solubilization criterion was interpreted in terms of the relative magnitudes of two critical concentrations, i.e., the critical concentration C^* at which the polymeric oil-in-oil (POO) emulsion is formed as a result of microphase separation and the critical concentration at which phase separation into the copolymer solution and the homopolymer solutions occurs.[4] As shown in the schematic diagram of Figure 2, if C^* is outside of the binodal surface of the four-component phase diagram (as shown at a point C_1^*), the solution is homogeneous at C^* so that the three polymer solutes cooperate for the microphase separation to result in the POO emulsion with the homopolymers solubilized into the respective phases of the block polymer. On the other hand, if C^* is inside the binodal surface (as shown at a point C_2^*), the phase separation into the copolymer solution and the homopolymer solutions takes place before C^* is reached. Consequently, the block copolymer forms an inherent domain structure undisturbed by the homopolymers. The shape of the binodal surface is strongly dependent on molecular weight, leading to the criterion which depends on molecular weight.

Table I
Summary of Sample Characterization

specimen	$\bar{M}_n \times 10^{-3}$ total	$\bar{M}_n \times 10^{-3}$ PI block	wt fraction of PI block
SI-8	200	26	0.13
SI-21	320	71	0.22
HPS	81		
HPI	16		

In this work we further study, quantitatively, by means of small-angle X-ray scattering (SAXS), the change of the microdomain structure of styrene–isoprene (SI) diblock polymers with the addition of homopolystyrene (HPS) and/or homopolyisoprene (HPI), which satisfy the solubilization criterion. We also study the effect of casting solvents on the domain structure. The block polymers studied in this work are all styrene rich so that they have the morphology of polyisoprene spheres dispersed in a polystyrene matrix. We will study changes in the domain radius, the interdomain distance, the size distribution, and the characteristic thickness of the interfacial region between the two coexisting polymer phases as a function of amount of the homopolymers blended in a binary mixture (HPS and SI) and a ternary mixture (HPS, HPI, and SI). All systems studied here are prepared by solvent casting with toluene and have the morphology of polyisoprene spheres in a polystyrene matrix.

II. Experimental Section

Table I is a summary of sample characterization. All specimens used were prepared by anionic polymerization, according to a

0024-9297/81/2214-0844$01.25/0

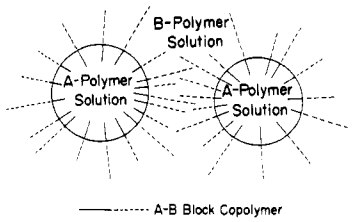

Figure 1. Polymeric oil-in-oil emulsion of A droplets in B solution.

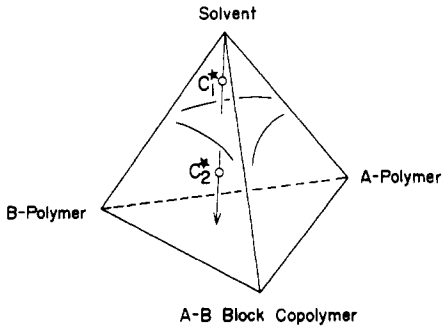

Figure 2. Schematic representation of the binodal surface in the phase diagram of a four-component system. C^* is the critical concentration for the formation of polymeric oil-in-oil emulsion.

method described in previous papers. The styrene–isoprene diblock polymers SI-8 and SI-21 are identical with those designated as SI-3 and SI-5 in the previous papers,[9,10] respectively. The molecular weights of homopolystyrene (HPS) and homopolyisoprene (HPI) are smaller than those of corresponding block molecular weights so that they satisfy the solubilization criterion.

A series of film specimens designated as the CO series was prepared by casting 10 wt % toluene solutions of the ternary polymer mixture of HPS, HPI, and SI-8 onto a glass plate. The homopolymers are blended on the isopleth line so that overall contents of styrene and isoprene are kept constant and equal to those of pure block polymer SI-8, i.e., 87 and 13 wt %, respectively. The specimen CO-90 designates the ternary mixture containing 90 wt % block polymer on the isopleth line (see Table II).

A series of film specimens designated as the BS series was also prepared by casting 10 wt % toluene solutions of the binary polymer mixture of HPS and SI-21. The specimen BS-10 designates the binary mixture containing 10 wt % HPS. A series of film specimens was also prepared by casting 10 wt % toluene, methyl ethyl ketone (MEK), and isopropyl acetate (IPA) solutions of SI-21 in order to investigate the effect of casting solvents on the microdomain structure. The solvent was very gradually evaporated at 30 °C for 1 week. The film specimens thus formed were further dried in a vacuum line of 10^{-6} torr until the specimens were at constant weight.

The microdomain structure in the solid film was investigated by electron microscopy by using the osmium tetraoxide fixation technique[11] and by SAXS techniques. The details of the techniques were described elsewhere,[12] and they will not be repeated here.

III. Results and Discussion

1. Domain Size and Interdomain Distance. Figure 3 shows the microdomain structure in the solvent-cast films of the ternary blends (a) and of the binary blends (b) as observed by transmission electron microscopy on ultrathin sections stained by OsO_4. It is obvious that all the systems have spherical microdomains composed of polyisoprene chains dispersed in a matrix of polystyrene chains. A close

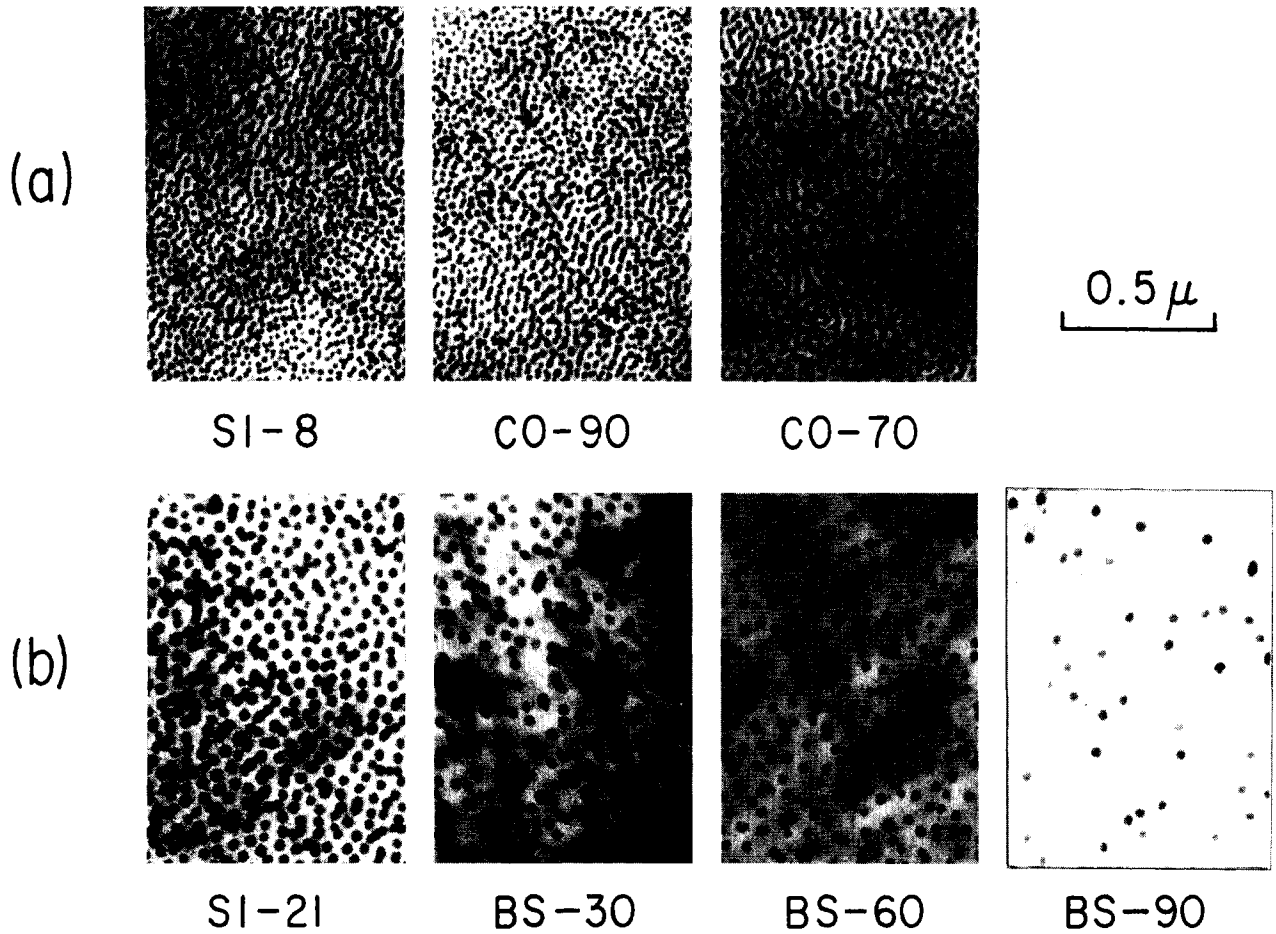

Figure 3. Microdomain structure in the solvent-cast films of the ternary blends (a) and of the binary blends (b) as observed by transmission electron microscopy on ultrathin sections stained by OsO_4.

Table II
Domain and Domain-Boundary Properties of the Binary and the Ternary Blends of the Block Copolymers with Corresponding Homopolymers

sample code	wt % PI	domain spacing $\bar{D}$, nm	domain radius $\bar{R}$, nm	domain radius $\sigma_r/\bar{R}$	interfacial properties ΔR, nm	interfacial properties f, %
SI-8	12.9	35.3 ± 1.8	9.4 ± 0.5	0.11 ± 0.01	1.7 ± 0.2	9.4 ± 1.9
CO-90	12.9	39.2 ± 2.0	10.8 ± 0.5	0.11 ± 0.01	2.1 ± 0.2	10.3 ± 2.1
CO-70	12.9	44.1 ± 2.2	11.5 ± 0.6	0.13 ± 0.01	2.0 ± 0.2	9.0 ± 1.8
SI-21	21.9	64.0 ± 3.2	17.1 ± 0.9	0.10 ± 0.01	2.0 ± 0.2	9.2 ± 1.8
BS-30	15.3	70.4 ± 3.5	15.5 ± 0.8	0.12 ± 0.01	1.7 ± 0.2	6.2 ± 1.2
BS-60	8.8	80.6 ± 4.0	14.2 ± 0.7	0.12 ± 0.01	1.8 ± 0.2	4.4 ± 0.9
BS-90	2.2					

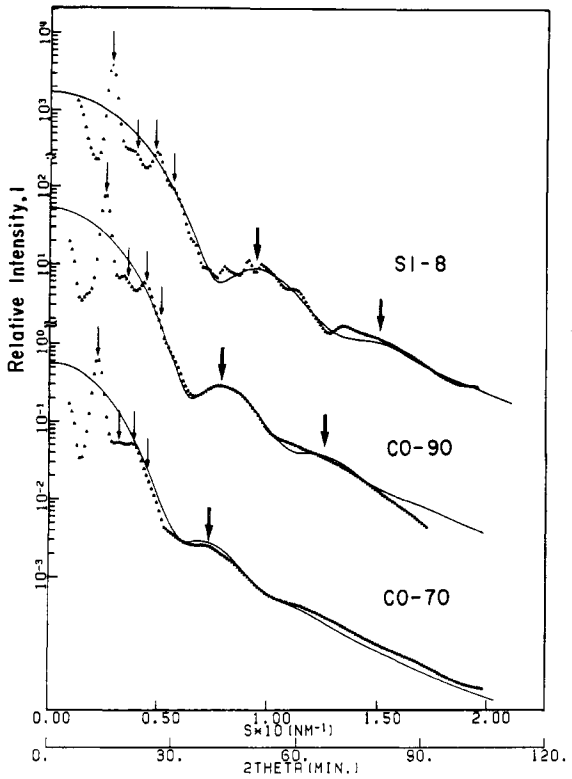

Figure 4. Desmeared small-angle X-ray scattering profiles for the SI block and its ternary blends. The measured profiles (plotted by triangles) were corrected for the background scattering I_b. The profiles drawn by lines are best-fitted independent scattering I_p from isolated spheres (see eq 2).

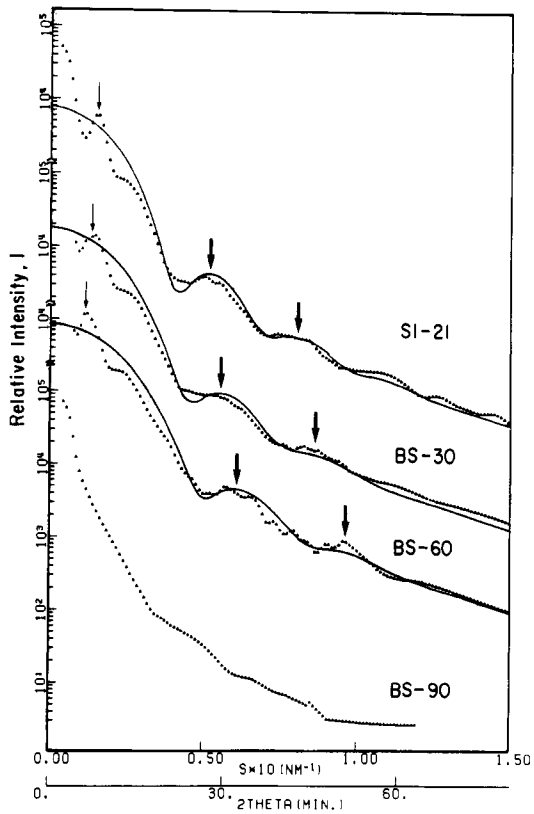

Figure 5. Desmeared small-angle X-ray scattering profiles for the SI block and its binary blends. The measured profiles (plotted by triangles) were corrected for the background scattering I_b. The profiles drawn by lines are best-fitted independent scattering I_p from isolated spheres.

inspection of the micrographs indicates that, with increasing content of the homopolymers, both the average radius of the spheres ($\bar{R}$) and the interdomain distance ($\bar{D}$) increase in the ternary systems (CO series), whereas $\bar{R}$ remains almost the same but $\bar{D}$ increases in the binary systems (BS series). The changes in $\bar{R}$ and $\bar{D}$ may be a consequence of solubilization of the homopolymers into the respective phases, as will be discussed later in a more quantitative manner.

The changes in $\bar{R}$, $\bar{D}$, and the size distribution σ_r upon blending the homopolymers are more quantitatively studied by means of SAXS. Figures 4 and 5 show the SAXS profiles for the ternary system and binary system, respectively. The profiles (plotted by triangles) were corrected for air scattering, absorption, and the collimation errors along the slit width and slit height. They were also corrected for the background scattering, I_b, arising from the thermal diffuse scattering within each phase; i.e., the corrected intensity I is obtained after subtracting I_b from the desmeared intensity I_{obsd}: $I = I_{obsd} - I_b$.

As discussed in detail in a previous paper,[10] the block polymers SI-8 and SI-21 have a long-range order in spatial arrangement of the spherical domains, a cubiclike macrolattice, giving rise to a number of interparticle interference maxima as shown by thin arrows. The first-order peak is associated with the average nearest-neighbor distance $\bar{D}$ between the spheres by Bragg's equation

$$2\bar{D} \sin \theta_m = \lambda \qquad (1)$$

where $2\theta_m$ is the scattering angle of the first-order peak and λ is the X-ray wavelength. There exist higher order scattering maxima at scattering angles $\sqrt{2}$, $\sqrt{3}$, and $\sqrt{4}$ of the first-order peak (see peaks labeled by thin arrows). The interdomain distance $\bar{D}$ was estimated by using eq 1 as a function of amount of the homopolymers blended, the results being summarized in Table II.

At larger scattering angles, the interference function approaches unity and the scattering from the system is capable of being described by independent scattering. The broad scattering maxima marked by thick arrows are associated with the scattering maxima from isolated spherical domains. The measured profiles were best fitted with the

calculated profiles $I_p(s)$ for the isolated spheres with a Gaussian size distribution

$$I_p(s) = \int_0^\infty dR\ P(R)f^2(s;R) / \int_0^\infty dR\ P(R) \quad (2)$$

$$P(R) = (\text{const}) \exp[-(R - \bar{R})^2/2\sigma_r^2] \quad (3)$$

where $\bar{R}$ is the average radius of the spheres, σ_r is its standard deviation, and $f^2(s;R)$ is the scattering factor from a sphere of radius R with a diffuse boundary region[9,10]

$$f(s;R) = E_e(\rho_1 - \rho_2)V\Phi(U) \exp(-2\pi^2\sigma^2s^2) \quad (4)$$

$$U = 2\pi Rs \qquad V = 4\pi R^3/3 \quad (5)$$

$$\Phi(U) = (9\pi/2)^{1/2}J_{3/2}(U)/U^{3/2} \quad (6)$$

$$s = (2 \sin \theta)/\lambda \quad (7)$$

where σ is the parameter associated with the thickness of the diffuse boundary, E_e is the scattering amplitude from a single electron, and ρ_1 and ρ_2 are, respectively, the electron densities of the spheres and their surrounding medium.

The best-fit curves for I_p with I are also included in Figures 4 and 5 (solid lines), which gave estimates for $\bar{R}$ and σ_r. The results are again summarized in Table II. It is clearly seen that the values $\bar{D}$ and $\bar{R}$ increase with increasing homopolymer fraction for the ternary system, whereas $\bar{D}$ increases but $\bar{R}$ decreases for the binary system. On the other hand, the relative value $\sigma_r/\bar{R}$ is essentially identical for all the specimens, indicating that the amount of homopolymer blended does not significantly perturb the size distribution of the domains. The changes in $\bar{R}$ and $\bar{D}$ may be an indication of the solubilization of the homopolymers into the respective phases of the block polymer, as discussed immediately below.

The interdomain distance D_0 and the radius of the domain R_0 for the pure block polymer system are interrelated to molecular volumes of polyisoprene block v_{BI} and polystyrene block v_{BS} and number of the block polymer chains per single domain N_{b0}

$$4\pi R_0^3/3 = N_{b0}v_{BI} \quad (8)$$

$$D_0^3/\epsilon_0 = N_{b0}(v_{BI} + v_{BS}) \quad (9)$$

where ϵ_0 is a constant associated with the spatial packing of the spheres composed of polyisoprene block chains. When the homopolymers are incorporated into the system, the system attains a new equilibrium to result in R_0, D_0, N_{b0}, and ϵ_0 being changed to R, D, N_b, and ϵ, respectively

$$4\pi R^3/3 = N_b v_{BI} + N_{HI}v_{HI} \quad (10)$$

$$D^3/\epsilon = N_b(v_{BI} + v_{BS}) + N_{HI}v_{HI} + N_{HS}v_{HS} \quad (11)$$

where N_{HI} and N_{HS} are number of homopolyisoprene (HPI) chains and homopolystyrene (HPS) chains solubilized into the block polymer domains and v_{HI} and v_{HS} are the molecular volumes of the respective homopolymers.

In our special case we can assume $\epsilon = \epsilon_0$ from the experimental data shown in Figures 4 and 5, the scattering profiles in the small s region being essentially unaltered by the amount of the homopolymers blended, except for peak broadening, as seen in Figure 5.

We define ψ_H, the volume fraction of the homopolymers in the mixture, as

$$\psi_H = \frac{N_{HI}v_{HI} + N_{HS}v_{HS}}{(N_{HI}v_{HI} + N_{HS}v_{HS}) + N_b(v_{BI} + v_{BS})} \quad (12)$$

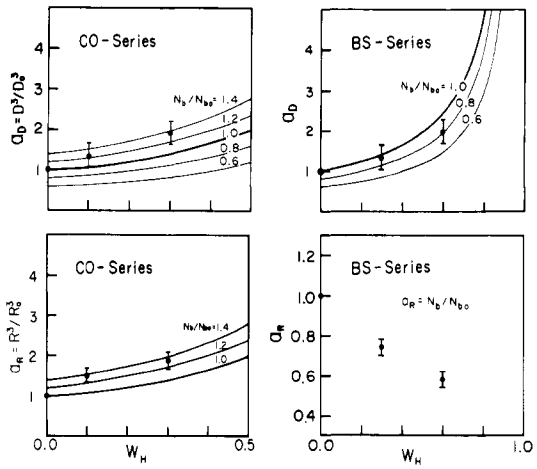

Figure 6. Changes in the ratios a_D and a_R as a function of W_H. The experimental values are shown by solid circles, while the calculated results are shown by lines for various values of N_b/N_{b0}.

By assuming that the homopolymers mixed are all solubilized into the respective phases, one can obtain that

$$a_D \equiv \left(\frac{D}{D_0}\right)^3 = \frac{N_b}{N_{b0}} \frac{1}{1 - \psi_H} \quad (13)$$

$$a_R \equiv \left(\frac{R}{R_0}\right)^3 = \frac{N_b}{N_{b0}} \left\{1 + \frac{\psi_H}{1 - \psi_H} \frac{\psi_{HI}}{\psi_{BI}}\right\} \quad (14)$$

where ψ_{HI} and ψ_{BI} are volume fractions of polyisoprene in the homopolymer mixture and in the block polymer, respectively; i.e.

$$\psi_{HI} = N_{HI}v_{HI}/(N_{HI}v_{HI} + N_{HS}v_{HS}) \quad (15)$$

$$\psi_{BI} = v_{BI}/(v_{BI} + v_{BS}) \quad (16)$$

For the ternary blends on the isopleth line (i.e., the CO series) it follows from eq 13 and 14 that

$$N_b/N_{b0} = a_D(1 - \psi_H) = a_R(1 - \psi_H) \quad (17)$$

since $\psi_{HI} = \psi_{BI}$. For the binary blends (BS series), $\psi_{HI} = 0$, so that

$$N_b/N_{b0} = a_D(1 - \psi_H) = a_R \quad (18)$$

The volume fraction of the homopolymers can be converted to the weight fraction W_H by assuming the densities of the polystyrene and polyisoprene phases are equal to those of the respective homopolymers, 1.052 and 0.925 g/cm^3.

Figure 6 shows changes in the ratios a_D and a_R as a function of W_H. The measured values are shown by solid circles, while the calculated results are shown by lines for various values of N_b/N_{b0}. The ratio N_b/N_{b0} is treated as a parameter in this analysis. For the ternary blend (CO series) the increase of the experimental values of a_D is equal to that of a_R within experimental error, which is in agreement with the prediction from eq 17. However, the rate of increase in the experimental values with W_H is higher than that expected for $N_b/N_{b0} = 1$. The value seems to increase from unity at $W_H \simeq 0$ to 1.2 or 1.4 with increasing W_H. With incorporation of the homopolymers, the system attains a new equilibrium in that the number N_b of block polymer chains per spherical domain increases. That is, the number of spherical domains tends to decrease and results in a smaller number of bigger spherical domains at a larger distance from each other to accommodate the homopolymers in the respective phases.

For the binary system (BS series) the experimental value of a_D increases with W_H, the rate of which, however, is

much slower than that expected for $N_b/N_{b0} = 1.0$. The value seems to decrease from unity at $W_H \simeq 0$ to 0.8 at $W_H = 0.6$, or even to 0.3 at $W_H = 0.9$. Corresponding to the decrease of the value a_D, the experimental values for a_R also decreases as seen in the figure. Therefore in contrast to the case of the CO series, the spherical domains tend to be divided into a greater number of smaller spheres with incorporation of the homopolystyrene into the matrix phase of the block polymer.

Why does the value N_b/N_{b0} change with W_H? This requires further studies, especially a statistical mechanical analysis of the ternary and binary systems, which are beyond the scope of this study. However, it might be worthwhile to discuss briefly two effects on the value of N_b/N_{b0}: (i) the effect of a partial (incomplete) solubilization of the homopolymers and (ii) the effect of nonequilibrium encountered in the solvent evaporation process.

A partial solubilization of the homopolymers into the respective domain phases in the block polymer makes the effective volume fraction ψ_H in eq 17 and 18 smaller. This results in the calculated value of a_D being smaller than those expected for a perfect solubilization for both ternary and binary systems, while it results in the calculated a_R being smaller than and equal to that expected for a perfect solubilization for the ternary and the binary systems, respectively. Therefore the partial solubilization tends to make the values N_b/N_{b0} (estimated by comparing experimental and calculated a_D and a_R values) larger than those expected for the perfect solubilization, at least, for the ternary system.

In our previous papers[10,13] we have discussed, in detail, equilibrium and nonequilibrium aspects of the spherical microdomains in block polymers. A nonequilibrium effect encountered in the solvent evaporation process tends to make the absolute values of $\bar{R}$, $\bar{D}$, and N_{b0} of the block polymers in the solid state much smaller than the equilibrium values. During the solvent evaporation process, the microdomain structure is formed at the critical concentration C^*. Upon further evaporation of solvent, the system attains a new equilibrium by changing the number N_{b0} of block polymer chains per domain, N_{b0} being increased so as to reduce the surface-to-volume ratio, i.e., to reduce energetic interactions between the two block chains.

In the spherical domain systems, N_{b0} can be changed only by a process involving a transport of A chains through the matrix B chains. This process must overcome a large energetic barrier which increases with increasing concentration, resulting in the domain morphology (i.e., the value N_{b0}) being fixed at a certain concentration level. The solvent further evaporates but the system cannot reach a new equilibrium. Thus further changes in $\bar{R}$ and $\bar{D}$ occur as a consequence of decreasing v_A and v_B, the molecular volumes. Such nonequilibrium effects should occur, in principle, even for the ternary and binary systems where, as in the pure block polymer systems, the estimated values of N_b in the solid state should be much smaller than the equilibrium value. Therefore one has to bear in mind this nonequilibrium effect to compare the experimental results with any equilibrium theories, although the effect may tend to cancel when one considers the ratio N_b/N_{b0} only. Experimental estimations of $\bar{R}$ and $\bar{D}$ as a function of concentration would be very useful to separate nonequilibrium and equilibrium aspects.

2. Domain-Boundary Thickness. Thickness of the interfacial region between the two coexisting phases, i.e., polyisoprene spheres and the polystyrene matrix, is evaluated as a function of W_H for the ternary and binary systems by analyzing the systematic deviation of the SAXS intensity distribution at large scattering angles from Porod's law[14] for the two-phase systems with a sharp boundary, i.e., zero interfacial thickness. We estimated the interfacial thickness on the basis of the full analysis on the smeared data, a new approach that we have proposed in our previous paper.[10] That is, the parameter σ associated with the interfacial thickness is estimated by a nonlinear curve fitting of $s^3\tilde{I}$ and $s^3\tilde{I}_{theor}$, where $\tilde{I}$ and $\tilde{I}_{theor}$ are the measured and theoretical smeared scattering profiles corrected for the background scattering $\tilde{I}_b$ (see Figures 10 and 11). The theoretical smeared intensity $\tilde{I}_{theor}$ is given, for a Gaussian slit-length weighting function $W_l(u)$, by[10]

$$I_{theor}(s) = (\text{const})s^{-3}\{[1 - 2s^2(p^2 + 4\pi^2\sigma^2)]\ \text{Erfc}\ [s(p^2 + 4\pi^2\sigma^2)^{1/2}]\ \exp(s^2p^2) + s(p^2 + 4\pi^2\sigma^2)^{1/2}\ \exp(-4\pi^2\sigma^2s^2)\} \quad (19)$$

where

$$\text{Erfc}\ (x) = \int_x^\infty dt\ \exp(-t^2)$$

$$W_l(u) = W_l(0)\ \exp(-p^2u^2) \quad (20)$$

The parameter σ determines the electron density variation $\eta(\mathbf{r})$ across the interfacial region

$$\eta(\mathbf{r}) = \rho(\mathbf{r}) * h(\mathbf{r}) = \int d\mathbf{x}\ \rho(\mathbf{x})h(\mathbf{r} - \mathbf{x}) \quad (21)$$

where $\rho(\mathbf{r})$ is the electron density variation of the system having zero interfacial thickness and $h(\mathbf{r})$ is assumed to be Gaussian with a variance σ^2, as employed by Ruland.[15]

$$h(\mathbf{r}) = (2\pi\sigma^2)^{-3/2}\ \exp(-r^2/2\sigma^2) \quad (22)$$

We define the characteristic interfacial thickness ΔR[10] as

$$\Delta R = (2\pi)^{1/2}\sigma \quad (23)$$

which is mathematically equal to the integral width of the smoothing function[10] $h(\mathbf{r})$ and which has a physical meaning given by

$$\Delta R = \rho_0/|d\eta(r)/dr|_{r=R} \quad (24)$$

where $\rho_0 = \rho_1 - \rho_2$, the electron density difference between the two phases.

Figures 7 and 8 show the smeared SAXS intensity profiles for the ternary and binary systems, respectively. The SAXS intensity tends to increase with increasing s in the large-angle region due to increasing contribution of the scattering from thermal diffuse scattering within each phase ("background scattering", $\tilde{I}_b$). The background scattering must be subtracted from the measured intensity $\tilde{I}_{obsd}$ to obtain the smeared intensity $\tilde{I}$ corrected for the background scattering. In this series of papers,[9,10,12,13,18,19] $\tilde{I}_b$ was estimated according to an empirical procedure proposed by Vonk[17] or Ruland[16] where $\tilde{I}_b$ is determined from the least-squares fit of the measured curve with an assumed function, a polynomial or an exponential function over a sufficiently wide angular range ($2\theta \simeq 120$–300 min or $s \simeq 0.23$–0.57 nm^{-1}).

In this paper we estimated the background scattering $\tilde{I}_b$ by a new method based on an additivity law of the background scattering; i.e., the background scattering of the block polymer is equal to a weighted average of the background scattering from the respective homopolymers

$$\tilde{I}_b = W_{PS}\,\tilde{I}_{PS} + W_{PI}\,\tilde{I}_{PI} \quad (25)$$

The additivity law, eq 25, was experimentally found at room temperature as shown in Figure 9, where the solid

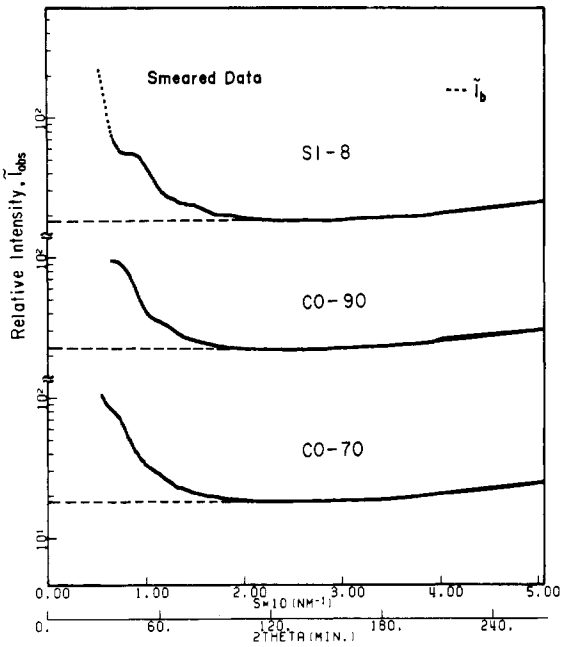

Figure 7. Smeared small-angle X-ray scattering profiles in the large s region for the ternary system (CO series). $\tilde{I}_b$ is the estimated background scattering.

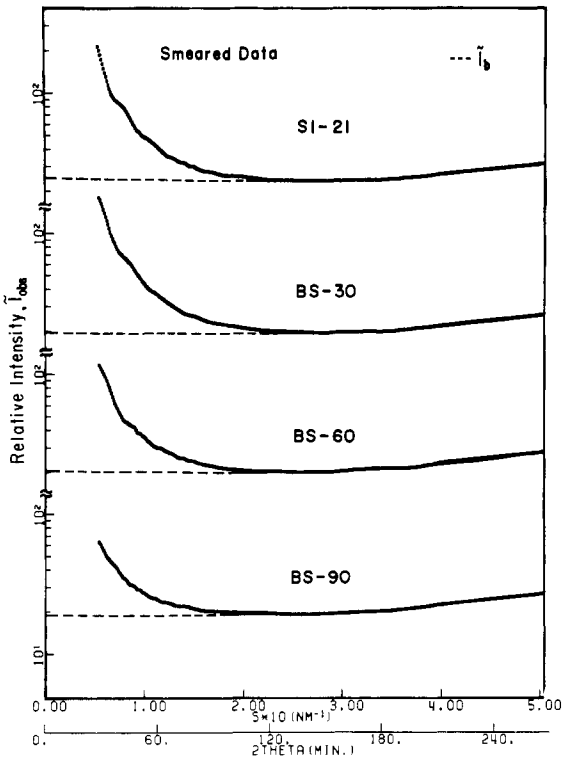

Figure 8. Smeared small-angle X-ray scattering profiles in the large s region for the binary system (BS series). $\tilde{I}_b$ is the estimated background scattering.

circles are measured intensity $\tilde{I}_{obsd}$ and the open circles are the estimated $\tilde{I}_b$ based on the additivity law of eq 25. The quantities W_{PS} and W_{PI} are the weight fractions of homopolystyrene and polyisoprene in the block polymer, respectively, and $\tilde{I}_{PS}$ and $\tilde{I}_{PI}$ are the background scatterings from the respective homopolymers. The agreement between the measured and calculated background scatterings is quite excellent. The figure also included the estimated $\tilde{I}_b$ based on the empirical procedure of Vonk (the solid curve), which also can be fitted to the measured curve.

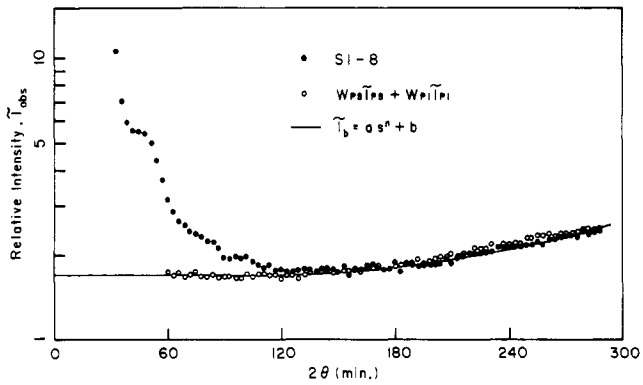

Figure 9. Smeared small-angle X-ray scattering profile in the large s region for SI-8 block polymer showing a method to estimate the background scattering $\tilde{I}_b$ based on the additivity law. The profile drawn by solid circles is for a measured profile of SI-8; the profile drawn by open circles is the one obtained by assuming an additivity of the background scattering from the homopolymers (eq 25) and that drawn by the solid line is the one obtained by assuming the polynomial $\tilde{I}_b = as^n + b$.

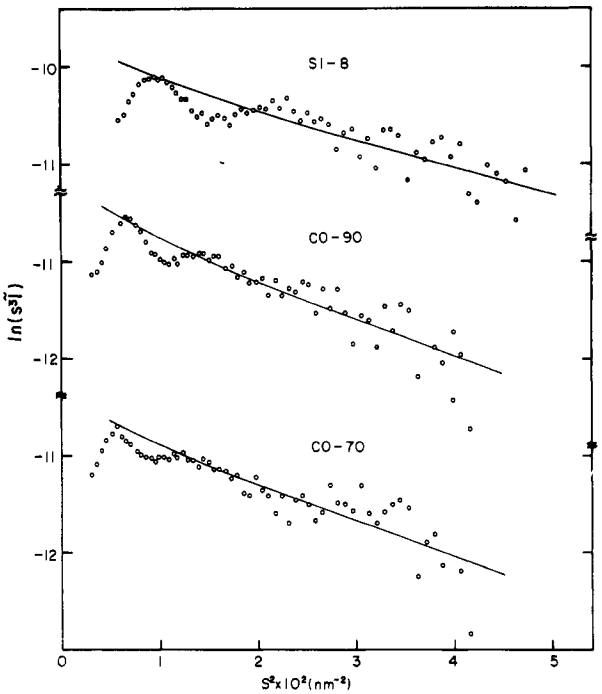

Figure 10. Plot of ln $(s^3\tilde{I})$ vs. s^2 to estimate the parameter σ associated with the characteristic interfacial thickness ΔR for the ternary system.

The background scatterings $\tilde{I}_b$ in Figures 7 and 8 (broken curves) are estimated on the basis of the additivity law of the background scattering.

Figures 10 and 11 show the plots ln $(s^3\tilde{I})$ vs. s^2 to estimate the value σ for the ternary and binary systems, respectively. The open circles are the measured values of $s^3\tilde{I}$ and the solid lines are the best-fitted results of $s^3\tilde{I}_{theor}$. From the σ values which give rise to the best fit, the ΔR are calculated, the results being summarized in Table II. The interfacial volume fraction f is also calculated from the measured values $\Delta R/\bar{R}$ and the volume fraction of the respective polymers (see eq 22 of ref 10), the results of which are also included in Table II.

Although there might be a small variation of ΔR with incorporation of the homopolymrs, especially in the case of the BS series, we can conclude that the characteristic interfacial thicknesses of all the systems are identical within experimental error (±10%). In our previous pa-

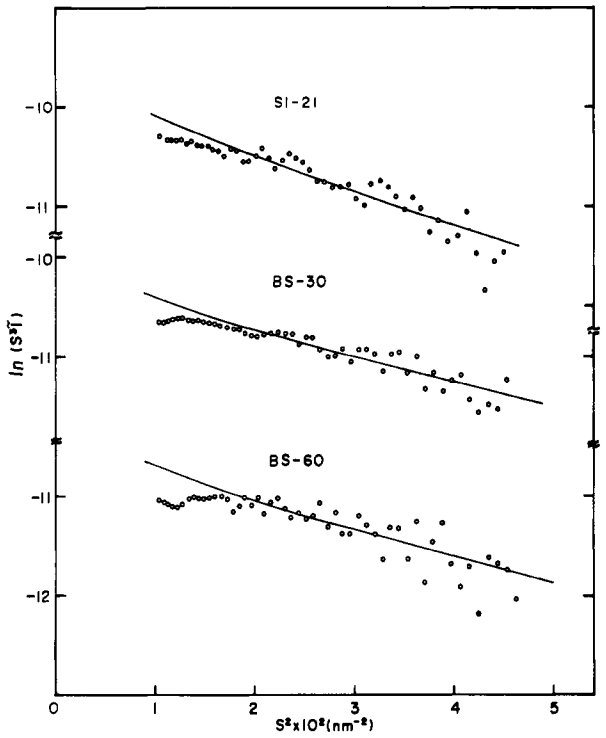

Figure 11. Plot of ln ($s^3\tilde{I}$) vs. s^2 to estimate the parameter σ for the binary system.

pers,[10,13,19] the ΔR values for the pure block polymers are shown to be in good agreement with the equilibrium theories developed by Helfand et al.[20,21] and Meier.[22] The overall interfacial volume is independent of the homopolymers mixed for the CO series, while it decreases with increasing the homopolystyrene for the BS series.

3. Interfacial Area. The constant (which will be defined as C in this section) in eq 19 is given by

$$C = (2\pi)^{-3}\pi^{1/2}I_e(\rho_1 - \rho_2)^2W_1(0)A_{int} \quad (26)$$

where I_e is the Thomson scattering intensity from an electron, $(\rho_1 - \rho_2)^2$ is difference of the electron density in the two-phases, and A_{int} is the interfacial area.

The interfacial thicknesses for BS-90 and a blend of HPS and HPI cannot be estimated with sufficient accuracy because the interfacial area A_{int} for such systems is very small so that the contribution of the scattering from the interfacial region becomes a very minor portion of the total intensity.

Form eq 19 and 26

$$\lim_{s\to 0}(s^3\tilde{I}_{theor}) = [I_eW_1(0)(\rho_1 - \rho_2)^2/16\pi^2]A_{int} \quad (27)$$

Thus from eq 27 one can evaluate a relative change of A_{int} with incorporation of the homopolymers. From the intercepts at $s = 0$ in the plots shown in Figure 12 one can estimate the change of the interfacial area relative to that of the block polymers, the results being summarized in Table III. It is shown that the interfacial area decreases with the homopolymers blended, the rate of the decrease being naturally much faster for the BS series than for the CO series.

For the spherical domain systems

$$A_{int} = (3\Psi_{PI}/\bar{R})V_t \quad (28)$$

where Ψ_{PI} is the overall volume fraction of polyisoprene chains forming the spherical domain of average radius of $\bar{R}$ and V_t is the irradiated volume of the sample. Thus the values $\bar{R}$ can be evaluated as a function of the homo-

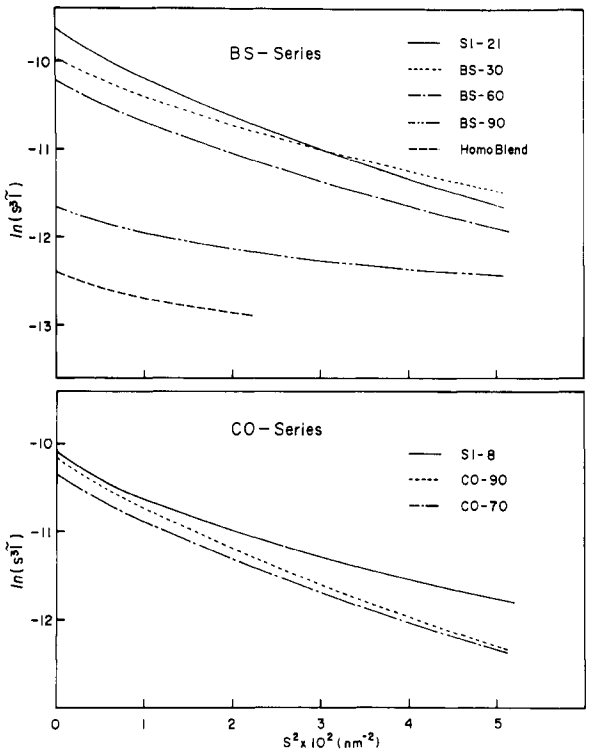

Figure 12. Plots of ln ($s^3\tilde{I}$) vs. s^2 for the binary blends (BS series) and for the ternary blends (CO series). The intercepts at $s = 0$ yield the relative change of A_{int} with incorporation of the homopolymers.

Table III
Interfacial Area A_{int} of the Binary and Ternary Systems Relative to Pure Block As Estimated from $\lim_{s\to 0}$ ln ($s^3\tilde{I}$)

sample code	A_{int}	$\bar{R}$,[a] nm	$A^b_{int,calcd}$	$\bar{R}^c_{calcd}$
SI-21	1	17.1[d]	1	17.1
BS-30	0.73 ± 0.14	16.6 ± 3.3	0.77	15.5
BS-60	0.57 ± 0.11	12.3 ± 2.4	0.50	14.2
BS-90	0.13 ± 0.02	13.6 ± 2.7		
blend	0.06 ± 0.01			
SI-8	1	9.4[d]	1	9.4
CO-90	0.96 ± 0.19	9.8 ± 1.9	0.87	10.8
CO-70	0.79 ± 0.16	11.9 ± 2.4	0.82	11.5

[a] Estimated from A_{int} from eq 28. [b] Estimated from $\bar{R}_{calcd}$. [c] Estimated from SAXS peak, as in Figures 4 and 5. [d] Values taken from $\bar{R}_{calcd}$.

polymers blended, the average radius $\bar{R}$ thus estimated being as follows: 9.4 (assumed), 9.8, and 11.9 nm for SI-8, CO-90, and CO-70, respectively, and 17.1 (assumed), 16.6, 12.3, and 13.6 nm for SI-21, BS-30, BS-60, and BS-90, respectively. These results are qualitatively in agreement with the values $\bar{R}$ (i.e., $\bar{R}_{calcd}$ in Table III) independently obtained from the SAXS peak (shown in Table II).

4. Effect of Casting Solvent on the Domain Properties. The effect of the casting solvents on the microdomain structure in the solid state was investigated for a particular block polymer, SI-21. As casting solvents, toluene, methyl ethyl ketone (MEK), and isopropyl acetate (IPA) were used, the solubility parameters of them being shown in Table IV. All film specimens obtained with these solvents have a spherical microdomain structure with a long-range order such as the one described in earlier sections. The radius of the domain $\bar{R}$ and the characteristic interfacial thickness ΔR were estimated by the method described in earlier sections, the results being summarized in Table IV.

Table IV
Effect of Casting Solvent on Spherical Microdomain of SI-21[a]

solvent	solubility parameter,[b] $(cal/cm^3)^{1/2}$	domain radius $\bar{R}$, nm	interfacial thickness ΔR, nm
toluene	8.9	17.1	2.0
methyl ethyl ketone	9.3	16.4	1.8
isopropyl acetate	8.4	16.5	1.8

[a] Solubility parameters for polyisoprene and polystyrene are 8.1 and 9.1 $(cal/cm^3)^{1/2}$. [b] From "Polymer Handbook".

Both the domain radius and the interfacial thickness are almost independent of the solvents used in this experiment for this particular block polymer. IPA is good solvent for polyisoprene in comparison to toluene and MEK. The values of $\bar{R}$ are again much less than the predicted values so that the nonequilibrium effect seems to be significant for these solvents also. The interfacial thickness ΔR also is independent of the solvent used. Thus the effect of solvent on the microdomain structure, if any, seems to vanish as the concentration increases.

IV. Concluding Remarks

For the particular polymer–solvent combinations studied in this work the solvent effects seem to vanish as concentration of the polymer increases, resulting in the final morphology in the solid state being hardly affected by the casting solvent. The solubilization of the homopolymers HPS and HPI into the SI block polymer domains is quantitatively studied. In the ternary blends of HPS, HPI, and SI, both the interdomain distance $\bar{D}$ and the radius $\bar{R}$ increase with increasing homopolymer volume fraction ψ_H, the result of which is interpreted as the ratio N_b/N_{b0} being increased with ψ_H (N_b and N_{b0} being the number of the block polymer chains per domain with and without homopolymers blended). On the other hand, in the binary blends of HPS and SI, $\bar{D}$ increases but $\bar{R}$ decreases with ψ_H, the results of which are interpreted as the ratio N_b/N_{b0} being decreased with ψ_H. Further investigation is required to clarify the change of the ratio N_b/N_{b0} and to separate equilibrium and nonequilibrium effects on that ratio. Upon blending of the homopolymer, the long-range order of the microdomains tends to be lost. The characteristic thickness of the interfacial region between the two coexisting phases is hardly changed over the amount of homopolymers blended in the study. Finally, we solved the uncertainty involved in subtracting the background scattering I_b (arising from thermal diffuse scattering within each phase) in the evaluation of the interfacial thickness ΔR. We found that the background scattering from the block polymers and their ternary and binary mixtures with the homopolymers are a weighted average of those from corresponding homopolymers. We were able to calculate and subtract the background scattering by using the additivity law.

Acknowledgment. Part of this work is supported by a Grant-in-Aid for Scientific Research from the Ministry of Education, Japan (449012), and by a scientific research grant through the Japan Synthetic Rubber Co. Ltd., Tokyo, Japan, and the Bridgestone Tire Co., Ltd., Tokyo, Japan.

References and Notes

(1) Riess, G.; Kohler, J.; Tournut, C.; Banderet, A. *Macromol. Chem.* **1967**, *101*, 58.
(2) Kohler, J.; Riess, G.; Banderet, A. *Eur. Polym. J.* **1968**, *4*, 173.
(3) Molau, G. E.; Wittbrodt, W. M. *Macromolecules* **1968**, *1*, 260.
(4) Inoue, T.; Soen, T.; Hashimoto, T.; Kawai, H. *Macromolecules* **1970**, *3*, 87.
(5) Molau, G. E. *J. Polym. Sci., Part A* **1965**, *3*, 1267, 4235.
(6) Molau, G. E.; Keskkula, H. *J. Polym. Sci., Part A-1* **1966**, *4*, 1595.
(7) Clayfield, E. J.; Lumb, E. C. *J. Colloid Interface Sci.* **1966**, *22*, 269.
(8) Meier, D. J. *J. Phys. Chem.* **1967**, *71*, 1861.
(9) Todo, A.; Uno, H.; Miyoshi, K.; Hashimoto, T.; Kawai, H. *Polym. Eng. Sci.* **1977**, *17*, 587.
(10) Hashimoto, T.; Fujimura, M.; Kawai, H. *Macromolecules* **1980**, *13*, 1659.
(11) Kato, K. *Polym. Eng. Sci.* **1967**, *7*, 38.
(12) Todo, A.; Hashimoto, T.; Kawai, H. *J. Appl. Crystallogr.* **1978**, *11*, 558.
(13) Fujimura, M.; Hashimoto, H.; Kurahashi, K.; Hashimoto, T.; Kawai, H., submitted to *Macromolecules* (Part 6 of this series).
(14) Porod, G. *Kolloid Z.* **1951**, *124* (2), 83. *Ibid.* **1952**, *125* (1), 51. *Ibid.* **1952**, *125* (2), 108.
(15) Ruland, W. *J. Appl. Crystallogr.* **1971**, *4*, 70.
(16) Rathie, J.; Ruland, W. *Colloid Polym. Sci.* **1976**, *254*, 358.
(17) Vonk, C. G. *J. Appl. Crystallogr.* **1973**, *6*, 81.
(18) Hashimoto, T.; Nagatoshi, K.; Todo, A.; Hasegawa, H.; Kawai, H. *Macromolecules* **1974**, *7*, 364.
(19) Hashimoto, T.; Shibayama, M.; Kawai, H. *Macromolecules* **1980**, *13*, 1237.
(20) Helfand, E.; Wasserman, Z. R. *Macromolecules* **1976**, *9*, 879.
(21) Helfand, E.; Wasserman, Z. R. *Macromolecules* **1978**, *11*, 960.
(22) Meier, D. J. *Prepr. Polym. Colloq., Soc. Polym. Sci., Jpn.* **1977**, 83.

Viscoelastic Properties of Aromatic Ionomers

M. Rigdahl, B. A. Reinhardt,[1] F. W. Harris,[1] and A. Eisenberg*
Department of Chemistry, McGill University, Montreal, Quebec, Canada H3A 2K6.
Received February 11, 1981

ABSTRACT: The dynamic mechanical properties and stress relaxation behavior in the solid state are studied for two aromatic ionomers. The ionomers are potassium salts of carboxylated-phenylated polyphenylenes. Mechanical loss tangent measurements indicate that the glass transition temperature is of the order 300 °C for both ionomers. The stress relaxation behavior in the primary transition is typical of an ionomer; i.e., a broad distribution of relaxation times is observed. It is concluded that even at temperatures higher than 300–320 °C, ionic interactions still persist and strongly influence the viscoelastic properties of the aromatic polymers. Some experiments on the dynamic mechanical properties of the aromatic ionomers at low temperatures are also reported.

Introduction

It is well-known that the presence of ions in polymers exerts a significant influence on the solid-state properties. In particular, the structure and the viscoelastic properties of ionomers often exhibit very complex behavior when ions are incorporated into the material. Consequently, a num-

0024-9297/81/2214-0851$01.25/0